

# Fast Transient Stability Prediction Using Grid-informed Temporal and Topological Embedding Deep Neural Network

Peiyuan Sun, Long Huo, Siyuan Liang, and Xin Chen

**Abstract**—Transient stability prediction is critically essential to the fast online assessment and maintaining the stable operation in power systems. The wide deployment of phasor measurement units (PMUs) promotes the development of data-driven approaches for transient stability assessment. This paper proposes the temporal and topological embedding deep neural network (TTEDNN) model to forecast transient stability with the early transient dynamics. The TTEDNN model can accurately and efficiently predict the transient stability by extracting the temporal and topological features from the time-series data of the early transient dynamics. The grid-informed adjacency matrix is used to incorporate the power grid structural and electrical parameter information. The transient dynamics simulation environments under the single-node and multiple-node perturbations are used to test the performance of the TTEDNN model for the IEEE 39-bus and IEEE 118-bus power systems. The results show that the TTEDNN model has the best and most robust prediction performance. Furthermore, the TTEDNN model also demonstrates the transfer capability to predict the transient stability in the more complicated transient dynamics simulation environments.

**Index Terms**—Deep Neural Network, Graph Convolution Network, Temporal Convolution Network, Transient Stability, Topological Embedding

## I. INTRODUCTION

**D**IGITALIZATION plays an essential role in the modernization of the power systems. The wide deployment of phasor measurement units (PMUs) enable the data collection on wide-area power systems and help engineers in utilizing large volumes of data, analyzing dynamic events in the grid, and the data-driven real-time transient stability prediction [1], [2]. Furthermore, the uncertainties of decentralized renewable energies demand a fast online assessment of transient stability [3]. Currently, the prediction methods of transient stability can be classified into two categories, *i.e.*, the model-driven methods and the data-driven methods [4].

One of the commonly used model-driven methods is the laborious Time-domain Simulation (TDS) based on high-dimensional nonlinear differential-algebraic equations (DAEs) that express the dynamics of power systems [5]. TDS is time-consuming since it demands the whole state trajectories to reveal the system stability. Although people have proposed different approaches to accelerate the TDS process, such as parallel computing [5], advanced hardware [6], *etc.*, huge computation resources are still required to handle the increasing complexity of power systems and diverse operational scenarios. The Lyapunov functions family's model-driven method is used for an analytical approach for stability assessment

in power systems [7], [8]. Unfortunately, finding a Lyapunov function to accurately evaluate the transient stability of power systems has been proved to be very difficult [9].

Recently, the data-driven methods, especially the deep learning approaches, attracted a lot of research interests on predicting transient stability in power systems [1], [2], [10], [11]. Compared with the model-driven methods, deep learning performance does not rely on the power systems' prior knowledge and model details. Furthermore, the strong generalization ability and the nature of offline training and online diagnosis pattern of deep learning provide great potentials to meet the high accuracy and fast online requirements in practical applications [12].

Among the existing deep learning models, Convolution Neural network (CNN) has made significant achievements in many fields [13], [14], including transient stability prediction in power systems. For example, Hou et al. [2] proposed a power system transient stability fast evaluation model based on CNN and the voltage phasor complex plane image. Rong Yan et al. [10] designed cascaded CNNs to capture data from different TDS time intervals, extract features, predict stability probability, and determine TDS termination. Besides, many other deep learning models are also used for predicting transient stability, such as auto-encoder [1], Long Short-Term Memory (LSTM) network [11], and Generative Adversarial Network (GAN) [15]. However, the architectures of the above deep learning models lack proper interpretability with the spatial correlations of power systems, given that, essentially, power systems are complex dynamical networks. Therefore, effectively using the important information of power network structures in deep learning remains a challenging problem.

The recently developed Graph Neural Network (GNN) is a promising deep learning model to extract features of the spatial correlations of power systems since GNN can naturally map the power network structure into its neural network architecture. As one of the GNN family, Graph Convolution Network (GCN) [16] combines topological structure with convolution algorithm and has been proved to be extremely powerful for the complex dynamical network analysis such as traffic prediction [17] and action recognition [18]. GCN demonstrates good classification and prediction capability with the graph-structured data in power systems [19], [20]. For example, Yuxiao Liu et al. [21] developed an interpretable GCN to guide cascading failure search efficiently. Nevertheless, the GCN is not adept at capturing the sequential characteristics, *i.e.*, the temporal information of time series of power system

dynamics. Additional techniques are needed to extract features from the time-domain of power system transient dynamics. For sequence modeling [22], the convolutional technique has been developed extensively in recent works and outperformed the baseline of well-known recurrent network architectures for sequence modeling tasks [23]. As one of the convolutional technique-based recurrent architectures, Temporal Convolutional Network [24], also known as TCN, has been utilized for time-series predictions in power systems, demonstrating powerful memory ability [25], [26]. In this paper, the temporal and topological embedding deep neural network (TTEDNN) model is proposed combining GCN and TCN to capture the spatio-temporal features of transient dynamics in power systems.

Generally, the main contributions of this paper are as follows:

- 1) The TTEDNN model is proposed to predict the transient stability by the temporal and spatial features extracted from the time-series data of the early transient dynamics. The grid-informed adjacency matrix is used to incorporate the power grid structural and electrical parameter information;
- 2) The performance of the TTEDNN model to predict the transient stability is highly efficient and accurate compared to existing deep learning methods and traditional TDS method;
- 3) The predictive capability of the TTEDNN model is robust. The TTEDN model trained with the second-order swing equations demonstrates good performance to predict the transient stability in more complicated transient dynamics simulation environments, *i.e.*, the higher-order (11th order) power system model.

The rest of this paper is organized as follows. Section II introduces simulation environment of transient dynamics. Section III proposes the architecture of the TTEDNN model. Case studies are given in Section IV. The transfer predictive capability is investigated in Section V. The conclusion remarks are drawn in Section VI.

## II. SIMULATION ENVIRONMENT OF TRANSIENT DYNAMICS

In this section, the power system models and perturbations of the transient dynamics simulation environment are described as follows.

### A. Models

The simulation environment of transient dynamics is set up for the data generation to train and test the TTEDNN model. The topology of a connected power system can be modelled as a weighted undirected graph  $G = (\mathcal{V}, \mathcal{E}, \mathbf{Y})$ , where  $\mathcal{V}$ ,  $\mathcal{E}$  and  $\mathbf{Y} \in \mathbb{C}^{N \times N}$  is the node set, edge set and the symmetric nodal admittance matrix, respectively. In graph  $G$ , nodes represent the generators or loads behind the buses and the edges represent the transmission lines. The notations of bus/node and transmission line/edge are used interchangeably. The number of nodes and edges are indicated by  $N$  and  $E$ , respectively. The swing equations, *a.k.a.*, the second-order

Kuramoto oscillators in physical community [27], are used in the simulation environment, which have been proved to be suitable to model the transient dynamics of power systems [28], [29]:

$$I_i \omega_{syn} \dot{\omega}_i + D_i \omega_i = P_{m,i} - \sum_{i \neq j} P_{ij}^{MAX} \sin(\delta_i - \delta_j) \quad (1)$$

where  $\delta_i \in \mathbb{S}^1$  and  $\omega_i \in \mathbb{R}^1$  are phase angle and angular frequency of node  $i \in \mathcal{V}$  with respect to power system rated frequency  $\omega_{syn}$ ,  $P_{m,i}$  is the mechanical power injection,  $P_{m,i} \geq 0$  for generator node and  $P_{m,i} \leq 0$  for load node,  $I_i > 0$  is the cumulative moment of inertia and  $D_i > 0$  is the damping coefficient. For the edge  $\{i, j\} \in \mathcal{E}$  between node  $i$  and node  $j$ ,  $P_{ij}^{MAX} = |V_i| \cdot |V_j| \cdot \Im(Y_{ij})$  is the maximum real power transfer capacity, where  $Y_{ij}$  denotes the element of  $\mathbf{Y}$ ,  $|V_i|$  and  $|V_j|$  are the voltage amplitude of node  $i$  and node  $j$ . Suppose the power system is lossless, only the imaginary part of admittance  $\Im(Y_{ij})$  is considered.

Dividing Eq. 1 by  $I_i \omega_{syn}$  and define  $\alpha_i = D_i / I_i \omega_{syn}$ ,  $P_i = P_{m,i} / I_i \omega_{syn}$  and  $K_{ij} = P_{ij}^{MAX} / I_i \omega_{syn}$ , the second-order power system model can be described as [30]

$$\begin{cases} \dot{\delta}_i = \omega_i \\ \dot{\omega}_i = -\alpha_i \omega_i + P_i + \sum_{i \neq j} K_{ij} \sin(\delta_j - \delta_i). \end{cases} \quad (2)$$

A higher order (11th order) power system model derived from the PST toolbox [31] is also considered in this paper, see reference book [32] for modelling details.

In this paper, we determine the transient stability in terms of synchronization in power systems [33]. For  $\gamma \in [0, \pi/2]$ , let  $\bar{\Delta}_G(\gamma) \subset \mathbb{T}^n$  be closed set of angle arrays  $(\delta_1, \dots, \delta_n)$  with the property  $|\delta_i - \delta_j| \leq \gamma$  for  $\{i, j\} \in \mathcal{E}$ . A solution  $(\delta, \omega) : \mathbb{R}_{\geq 0} \rightarrow (\mathbb{T}^n, \mathbb{R}^n)$  to the power system model of a given initial state in Eq. 2 is said to be synchronized if  $\delta(0) \in \bar{\Delta}_G(\gamma)$ ,  $\delta(t) = \delta(0)$  and  $\omega(t) = 0_n$  for all  $t \geq 0$ . In other words, here, synchronized trajectories have the properties of *frequency synchronization*, that is, all oscillators rotate with the same synchronization frequency  $\omega_{syn}$  and all their phases belong to the set  $\bar{\Delta}_G(\gamma)$  [29].

### B. Perturbations

The perturbations in power systems have varieties of sources including load variations, market trading, renewable energy fluctuations [34], *etc.* For example, energy trading happens at most of the time, inducing several considerable local frequency deviations per day, even as four times per hour. Physically, the perturbations in a dynamical system can be regarded as the initial states apart from the original stable equilibrium. Theoretical studies usually consider the distribution of power system frequency fluctuations as uniform or normal, which are not in line with the real situation. The distribution of the frequency in realistic power systems [35] demonstrates the non-Gaussian characteristics of heavy tail and skewness, which can be more accurately described by the Lévy-stable distribution. Additionally, maximum fluctuations of frequency should be also set to an appropriate value, otherwise the

perturbations will be too small to disturb the system or too large to be found in the realistic power systems. Normally, the perturbations of frequency  $\Delta f$  is bounded to  $\pm 1\%$  to  $\pm 4\%$  of rated frequency (50Hz or 60Hz) [36]. We set the perturbation limit of angular frequency as  $\Delta\omega = \Delta f = 20\text{rad/s}$ . We define  $m < N$  be the number of nodes simultaneously perturbed, where  $m = 1$  and  $m > 1$  refers to the single-node perturbations case and the multiple-node perturbations case, respectively.

### III. TEMPORAL AND TOPOLOGICAL EMBEDDING DEEP NEURAL NETWORK

Given perturbations and power network structures, the temporal and topological features embedding in the transient dynamics in power systems is crucial to the transient stability. The TTEDNN model is proposed to predict the transient stability in power systems by extracting the spatial and temporal features from the time series data generated with the transient dynamics effectively. The TTEDNN structure is shown in Fig. 1.

#### A. Data Representation

The transient dynamics of power system is represented as the multivariate time series data of angular frequency, denoting as  $\Omega_s = [\omega_1; \omega_2 \cdots \omega_i \cdots \omega_N]^T$ , where  $N$  is the number of nodes in power systems,  $\omega_i = [\omega_0^i; \omega_1^i; \cdots; \omega_j^i; \cdots; \omega_T^i]$  is the time series of the frequency of node  $i$  and  $T$  is the length of time series. The label  $y$  for  $\Omega_s$  is binary, i.e.,  $y = 1$  and  $y = 0$  for the initial states of  $\Omega_s$  will lead to a stable steady-state and unstable steady-state, respectively. In the TTEDNN prediction output gives the probability  $p$  that the power system will evolve to the stable steady-states or unstable steady-states. Numerically, we take  $p > 0.5$  for the stable steady-state and  $p \leq 0.5$  for the unstable steady-state.

#### B. Structure of TTEDNN

The TTEDNN structure has three main parts, the Graph Convolution (GC) modules, Temporal Convolution (TC) module and Multi-Layer Perception (MLP) prediction layer.

**GC Modules.** TTEDNN starts with the  $n$  GC modules to extract the topological features. Each GC module is composed of GCN layer, Batch Normalization (BN) layer and rectified linear unit (ReLU) [37] activation function sequentially.

The structure of the GCN layer can be represented as an undirected graph [16]  $G = (\mathcal{V}, \mathcal{E}, \mathbf{B})$ , where  $\mathcal{V} \in \mathbb{R}^N$  is the set of neurons,  $\mathcal{E} \in \mathbb{R}^E$  is the set of links between neurons and  $\mathbf{B} \in \mathbb{R}^{N \times N}$  is the adjacency matrix of the graph. The re-normalized adjacency matrix  $\hat{\mathbf{B}}$  is often used in the GCN layer:

$$\hat{\mathbf{B}} = \hat{\mathbf{D}}^{-1/2} \hat{\mathbf{B}} \hat{\mathbf{D}}^{-1/2} \quad (3)$$

where  $\hat{\mathbf{B}} = \mathbf{B} + \mathbf{I}_N$  denotes the adjacency matrix with self-loop, where  $\mathbf{I}_N$  is the identity matrix.  $\hat{\mathbf{D}}$  represents the diagonal node degree matrix where  $\hat{D}_{i,i} = \sum_j \hat{B}_{i,j}$ .

The operation of the  $i^{\text{th}}$  GC module is defined as

$$\mathbf{H}^{i+1} = \sigma(\mathbf{B}\mathbf{N}(\hat{\mathbf{B}}' \mathbf{H}^i \mathbf{W}^i + \mathbf{b}^i)) \quad (4)$$

where  $\sigma(\cdot)$  is the activation ReLU function,  $\mathbf{H}^{i+1} \in \mathbb{R}^{N \times C}$  denotes the output states of  $i^{\text{th}}$  GC module as well as the input states of  $(i+1)^{\text{th}}$  GC module,  $\mathbf{W}^i \in \mathbb{R}^{C \times F}$  is the network weight of GCN layer,  $\mathbf{b}^i \in \mathbb{R}^{N \times F}$  denotes bias. Then the last  $n^{\text{th}}$  GC module is connected to a flatten layer to reshape the output states. Following the flatten layer, a fully-connected (FC) layer is adopted to extract the topological features to feed into the TC module.

**TC Module.** As the GC modules extracting the topological features, the TC module is used to extract the temporal features. As shown in Fig. 1, the TC module is composed of  $R$  residual blocks using 1D fully convolutional network (FCN) [38]. 1D-FCN utilizes casual convolution technique and dilated convolution technique as well as a residual connection. The solely 1D-FCN structure produces an output with the same length of its input, and the casual convolution technique ensures that the output emitted by a 1D-FCN layer at time step  $t$  is convolved only with elements from time step  $t$  and earlier in the previous layer. Therefore, the TC module takes the whole history information into consideration for the future prediction. The disadvantage is that casual convolution technique can only look back to the historical information with the size linear to the network depth. The casual convolution can be optimized with the dilated convolution technique by introducing the exponential receptive field. Therefore, the TC module can take all historical information into account with smaller network depth. Specifically, the dilated convolution operation  $F(\cdot)$  can be defined as a dilated transformation of a 1-D time series data  $\mathbf{x}$ :

$$F(j) = \sum_{i=0}^{k-1} f(i) \cdot x_{j-d \cdot i} \quad (5)$$

where  $f(i)$  is the convolution filter  $f: 0, \dots, k-1 \rightarrow \mathbb{R}$ ,  $k$  denotes the filter size,  $d$  denotes the dilated factor and  $j = 1, \dots, n$  and  $n$  is the size of the  $\mathbf{x}$ . Adjusting dilation size can allow the top level of 1D-FCN represent a wider range of the input as much as possible, thus expand the receptive field extensively. Moreover, residual connection is used to stabilize the network training to make the layers to learn deep residual information as the modifications to the identity mapping when the casual convolution is dilated with considerable depth. As a result, the  $r^{\text{th}}$  residual block is defined as follows:

$$\mathbf{z}^r = \sigma(\mathbf{x}^r + LF(F(\mathbf{x}^r))) \quad (6)$$

where  $\mathbf{x}^r$  and  $\mathbf{z}^r$  denote the input and output of the  $r^{\text{th}}$  residual block respectively,  $r = 1, \dots, R$ ,  $LF(\cdot)$  denotes layer normalization technique [39].

**MLP Prediction Layer.** Finally, MLP with the sigmoid activation function is utilized to generate the prediction as a probability function.

**Grid-informed Adjacency Matrix.** Taking the electrical and structural properties of power system into consideration, three grid-informed adjacency matrices  $\mathbf{B}$  are proposed in the GC modules for the spatial features extraction. First, according

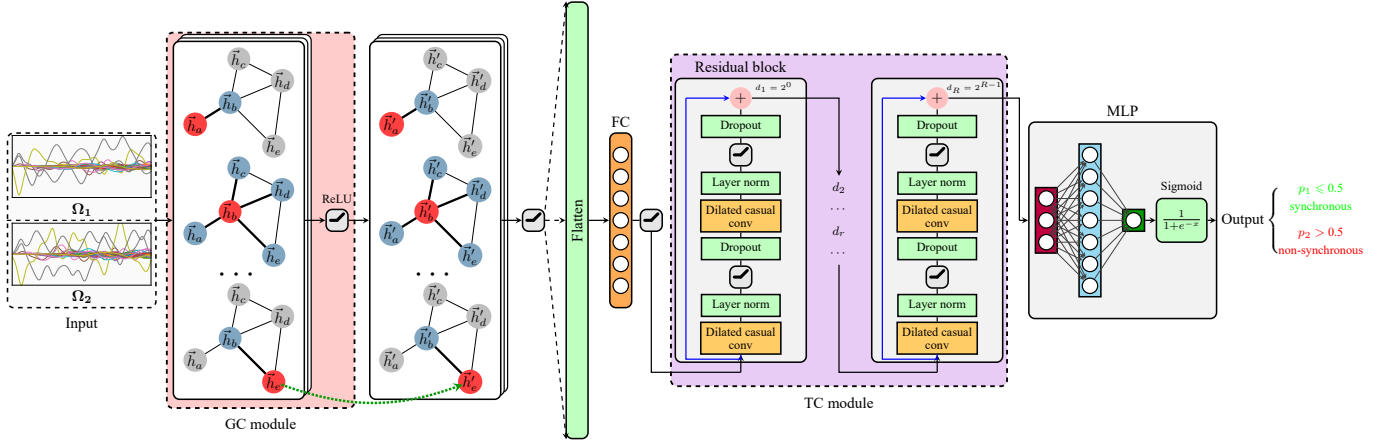


Fig. 1. Diagram of the TTEDNN structure.

to [16], we choose the binary adjacency matrix of power system added with self-connection, denoted as  $\mathbf{B}^I$  in Eq. 7. It considers the topology of power system, but ignores the weight of edges. Second, active power flows are added as the weights of edges in the adjacency matrix, denoted as  $\mathbf{B}^{II}$  in Eq. 8. Third, we treat the maximum transmission capability of a transmission line as off-diagonal elements in the adjacency matrix, together with active power injections for diagonal ones, denoted as  $\mathbf{B}^{III}$  in Eq. 9.

$$B_{ij}^I = \begin{cases} 1 & (i, j) \in \mathcal{E} \text{ or } i = j \\ 0 & (i, j) \notin \mathcal{E} \end{cases} \quad (7)$$

$$B_{ij}^{II} = \begin{cases} K_{ij} \sin(\delta_i - \delta_j) & (i, j) \in \mathcal{E} \\ 0 & (i, j) \notin \mathcal{E} \end{cases} \quad (8)$$

$$B_{ij}^{III} = \begin{cases} K_{ij} & (i, j) \in \mathcal{E} \\ 0 & (i, j) \notin \mathcal{E}, i \neq j \\ P_i & i = j \end{cases} \quad (9)$$

**Class Weighted Loss Function.** In the training of the TTEDNN model, the class weighted binary cross entropy (BCE) is used as the loss function with the  $L_2$  regularization defined as

$$\begin{aligned} Loss = & \sum_i (\alpha_1 y_i \log p_i + \alpha_0 (1 - y_i) \log(1 - p_i)) \\ & + \beta \sum_{k=1}^M \frac{1}{2} (\|w_k\|^2 + \|b_k\|^2) \end{aligned} \quad (10)$$

where  $y_i$  denotes the label and  $p_i$  denotes the model output of the  $i$ th sample,  $\alpha_0$  and  $\alpha_1$  represent weight factors corresponding to the stable state (frequency is synchronous at steady-states) and the unstable state (frequency is non-synchronous at steady-states), respectively. Additionally,  $w_k$  and  $b_k$  serve as learnable network parameters,  $\beta$  is the regularization weight.

Class-weighted BCE is adopted for the loss function and proved significantly helpful for the training dataset with the great imbalance of stability and instability. The imbalance of the dataset results from the fact that the power systems are

globally stable under the most initial state perturbations. There are more (less) stable (unstable) states samples in the dataset.

## IV. CASE STUDIES

### A. Simulation Data

The transient dynamics simulation environment is set up with the second-order power system model discussed in Section II. The simulation is solved by 4th order Runge-Kutta method with time step size  $\Delta t = 0.0125s$ . The IEEE 39-bus [40] and IEEE 118-bus [41] power systems are used for training and testing the TTEDNN model. The corresponding electrical parameters are obtained from MATPOWER 6.0 toolbox [42].

The training dataset contain the set of  $\Omega_s$  under the single-node perturbations. The test dataset consists of the set of  $\Omega_s$  and the corresponding label  $y$  under the single-node and multiple-node perturbations. For the dataset under the single-node perturbations, the initial states are randomly sampled  $\mathcal{K}_i$  times for all the nodes  $i = 1, \dots, N$  individually according to the uniform distribution of frequency. As for the dataset under the  $m$  multiple-node perturbations, since there are too many choices of  $m$  multiple nodes,  $M$  combinations of  $m$  multiple nodes are selected. For each combination, the initial states of  $m$  nodes are randomly sampled  $\mathcal{K}_m$  times according to the uniform distribution of frequency. For the dataset of single-node perturbations of the IEEE 39-bus power system, given  $\mathcal{K}_i = 1000$ ,  $i = 1, \dots, 39$ , 39000 samples in total are generated with 35349 stable samples and 3651 unstable samples. For the single-node perturbations dataset of the IEEE 118-bus system, given  $\mathcal{K}_i = 441$ ,  $i = 1, \dots, 118$ , 52038 samples in total are generated with 50754 stable samples and 1284 unstable samples. For the multiple-node perturbations dataset of the IEEE 39-bus power system, given  $m = 3$ ,  $M = 60$  and  $\mathcal{K}_m = 1000$ , 60000 samples in total are generated with 43888 stable samples and 16112 unstable samples. For the multiple-node perturbations dataset of the IEEE 118-bus power system, given  $m = 3$ ,  $M = 60$  and  $\mathcal{K}_m = 200$ , 12000 samples in total are generated with 11132 stable samples and 868 unstable samples. The dataset is divided into the training, validation and test datasets. 60% of the single-node dataset is used for the

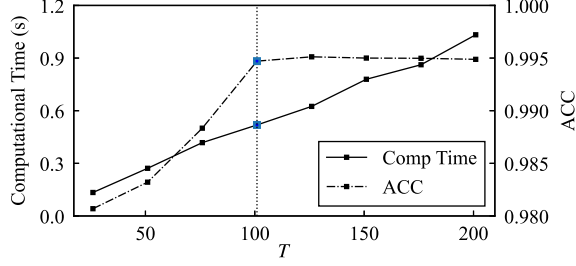


Fig. 2. ACC and computational time on the test dataset for different time series length in the IEEE 39-bus power system.

training, 20% of the single-node dataset is for the validation, and the remaining 20% of the single-node dataset and all the multiple-node dataset are combined for the test dataset.

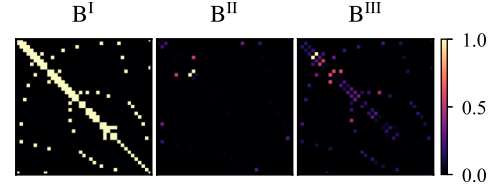
### B. Performance Analysis

The four metrics, ACC, Fall-out (FPR), Miss Rate (FNR), and AUC are used to measure the performance of the TTEDNN model, where  $ACC = \frac{TP+TN}{TP+TN+FP+FN}$ ,  $FPR = \frac{FP}{FP+TN}$ ,  $FNR = \frac{FN}{FN+TP}$ , and  $AUC = \int_0^1 TPR dFPR$  where TP is the true positive, TN is the true negative, FP is the false positive, FN is false negative, ACC denotes the prediction accuracy rate, TPR denotes true positive rate, FPR denotes false positive rate, TNR denotes true negative rate and FNR denotes false negative rate.

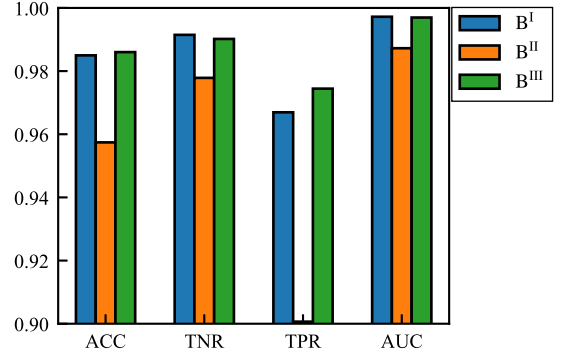
In order to understatement the optimal length of time series, ACC and computational time are calculated with different length  $T$  in Fig. 2. ACC increases to the maximum around  $T \approx 100$  while the computational time monotonically increases. Thus, 101 is chosen to be the optimal length  $T^*$  for the TTEDNN model.

The three grid-informed adjacency matrices in Eq. 7 to Eq. 9 are visualized in Fig. 3a. The performance measurements in terms of the four metrics of ACC, TNR, TPR, and AUC are evaluated for the three grid-informed adjacency matrices,  $B^I$ ,  $B^{II}$ , and  $B^{III}$ , respectively. The adjacency matrix  $B^{II}$  shows the worst performance as shown in Fig. 3b. The visualization in Fig. 3a shows that the adjacency matrix  $B^{II}$  is very sparse compared with the other two, which means that  $B^{II}$  discards the useful information about the power system topology and electrical properties. The performance measurements of  $B^I$  and  $B^{III}$  are almost the same, while  $B^{III}$  is slightly better on TPR. Hence, the grid-informed adjacency matrix  $B^{III}$  is used for the GC modules.

We train and test the TTEDNN model using Tensorflow 2.3.1 [43] and running on a server with Intel(R) Xeon(R) CPU E5-2620 v3. The TTEDNN model are tuned and validated according to the training score and validation score on the training and validation datasets. Two GC modules ( $n = 2$ ) with the same kernel size of 16 are used to extract topological features. The dimension of the FC layer is (64, 1). The TC module has five residual blocks ( $R = 5$ ) and exponential dilated factors  $d = 2^{r-1}$  for  $r = 1, \dots, R$  with kernel size  $k=2$  and the number of filters are 32. The MLP prediction layer



(a) Visualization of grid-informed adjacency matrices



(b) Performance in terms of ACC, TNR, TPR and AUC

Fig. 3. Visualization and performance comparison of three grid-informed adjacency matrices, (a) shows the visualization of three grid-informed adjacency matrices. (b) shows performance comparison of three grid-informed adjacency matrices on the multiple-node test dataset.

has the dimensions of (32, 1), (32, 1) for the input layer and the hidden layer respectively. The learning rate and batch size for the training are set to be  $1e^{-3}$  and 256.  $L_2$  regularization weight  $\beta$  is set to  $5e^{-4}$ . Weight factor  $\alpha_0$  is set to 1, and  $\alpha_1$  is calculated on each batch as

$$\alpha_1 = \begin{cases} 256 / \sum_{i=1}^{256} y_i - 1 & \sum_{i=1}^{256} y_i \neq 0 \\ 0 & \sum_{i=1}^{256} y_i = 0. \end{cases} \quad (11)$$

### C. Prediction Performance

Fig. 4 shows the ACC and Loss change at the different training epochs with the validation dataset. It can be found that the training of the TTEDNN model converges quickly and smoothly. ACC increases sharply to 98% within 20 epochs.

Table I shows the performance of the transient prediction under the single-node perturbations for the IEEE 39-bus and IEEE 118-bus power systems. The test performance under the single-node test dataset shows that the TTEDNN model outperforms all the existing deep learning methods including CNN [44], Attention-CNN [45], GCN [21], Graph Attention Network (GAT) [46] and Node-Level GCN (NGCN) [47]. The TTEDNN model has the best performance in terms of the ACC of 99.38% and the AUC of 0.9994 for the IEEE 39-bus power system, and the ACC of 99.88% and the AUC of 0.9999 for IEEE 118-bus power system. The correct prediction of unstable states is the critically important in the practical

TABLE I  
STABILITY PREDICTION UNDER THE SINGLE-NODE PERTURBATIONS IN THE IEEE 39-BUS AND THE IEEE 118-BUS POWER SYSTEMS.

Scenario	IEEE 39-bus				IEEE 118-bus			
	ACC(%)	FNR(%)	FPR(%)	AUC	ACC(%)	FNR(%)	FPR(%)	AUC
CNN	98.36	0.86	9.33	0.9907	99.62	0.23	5.78	0.9928
Attention-CNN	98.45	0.97	7.24	0.9930	99.69	<b>0.14</b>	6.64	0.9845
GCN	96.19	3.33	18.53	0.9558	99.25	0.18	2.15	0.9978
GAT	98.15	2.20	8.91	0.9852	99.53	0.18	6.14	0.9921
NGCN	84.27	10.36	12.17	0.8921	87.43	8.98	13.24	0.9135
Proposed TTEDNN	<b>99.38</b>	<b>0.65</b>	<b>0.36</b>	<b>0.9994</b>	<b>99.88</b>	0.17	<b>0.00</b>	<b>0.9999</b>

TABLE II  
STABILITY PREDICTION UNDER THE MULTIPLE-NODE PERTURBATIONS IN THE IEEE 39-BUS AND THE IEEE 118-BUS POWER SYSTEMS.

Method	IEEE 39-bus				IEEE 118-bus			
	ACC(%)	FNR(%)	FPR(%)	AUC	ACC(%)	FNR(%)	FPR(%)	AUC
CNN	80.73	11.93	39.68	0.7976	98.18	0.34	20.74	0.9601
Attention-CNN	82.49	16.16	21.27	0.7620	95.90	2.43	25.46	0.8942
GCN	93.21	2.31	10.45	0.9110	98.36	0.87	11.52	0.9814
GAT	90.26	11.66	4.41	0.9794	97.06	0.52	10.34	0.9956
NGCN	81.27	15.56	18.29	0.7821	86.62	13.21	16.43	0.8512
Proposed TTEDNN	<b>98.60</b>	<b>0.98</b>	<b>2.56</b>	<b>0.9970</b>	<b>99.08</b>	<b>0.09</b>	<b>9.33</b>	<b>0.9878</b>

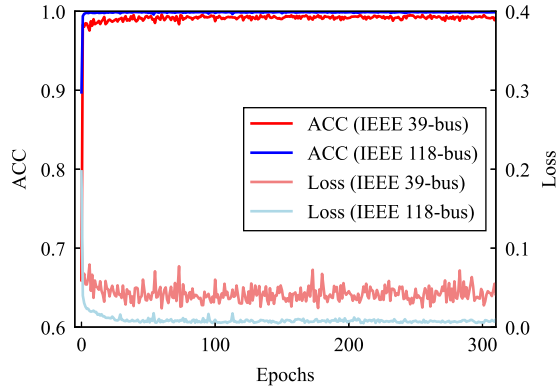


Fig. 4. ACC and class-weighted loss function *v.s.* epochs. The performance of the trained TTEDNN model on the validation dataset in terms of ACC and loss function for the IEEE 39-bus power system.

implementation, thus we pay much attention to *FPR*, which represents the proportion of the correct prediction in all unstable samples. The TTEDNN model has the best FPR with only 0.36%, *i.e.*, among all the 730 unstable samples, only three samples are mistaken predicted to be stable. Using the single-node test dataset of IEEE 118-bus power system, the attention-CNN method has the best FPR with 0.14%, slightly better than the TTEDNN model with 0.17%.

The prediction performance on the multiple-node test dataset is also investigated since the multiple-node perturbations make the prediction task more complicated. Compared with the performance of the transient stability prediction under

the single-node perturbations in Table I, the TTEDNN model still has the best performance in Table II as the ACC of 98.60% and the AUC of 0.9970 for the IEEE 39-bus power system and the ACC of 99.08% and the AUC of 0.9878 for the IEEE 118-bus power system. However, the existing deep learning methods show 3%-18% drop in ACC and AUC, while the TTEDNN model only has very small changes in terms of ACC and AUC. Clearly the TTEDNN model is much more robust than the existing deep learning methods.

The ACC in Table I and Table II indicates that the predictions of the TTEDNN model are highly close to the results of TDS method. Meanwhile, based on the Intel(R) Xeon(R) CPU E5-2620 v3 CPU, it takes approximately 0.5s and 5s for the trained TTEDNN model and the TDS method to forecast the transient stability, respectively, which indicates the TTEDNN model is 10 times faster than the TDS method.

## V. TRANSFER PREDICTIVE CAPABILITY

If the simulation can provide the sufficient information of the system behavior, the predictive model can learn from the simulation environment to make predictions. Learning from the simulation can be useful in the few-shot learning. The availability of the transient dynamics data in the realistic power system is rare, particularly the data on the unstable transient dynamics. When the transient dynamics data in the realistic power system is missing, we can build the rigorous simulation environment of higher-order transient dynamics by the MATLAB PST toolbox [31]. With the simulation environment, we can test the transfer capability of the TTEDNN model trained on the dataset generated with the coarse-grained simulation environment in Section IV-A. The second-order power system



TABLE III  
THE TRANSFER CAPABILITY FOR THE IEEE 39-BUS POWER SYSTEM  
FOR THE TWO TYPES OF THE SYNCHRONOUS AND CONSTANT  
IMPEDANCE UNDER SINGLE-NODE PERTURBATIONS.

Scenario	ACC(%)	FNR(%)	FPR(%)	AUC
Constant impedance	62.38	<b>0.00</b>	86.41	0.5001
Synchronous	<b>91.07</b>	15.32	<b>5.02</b>	<b>0.9707</b>

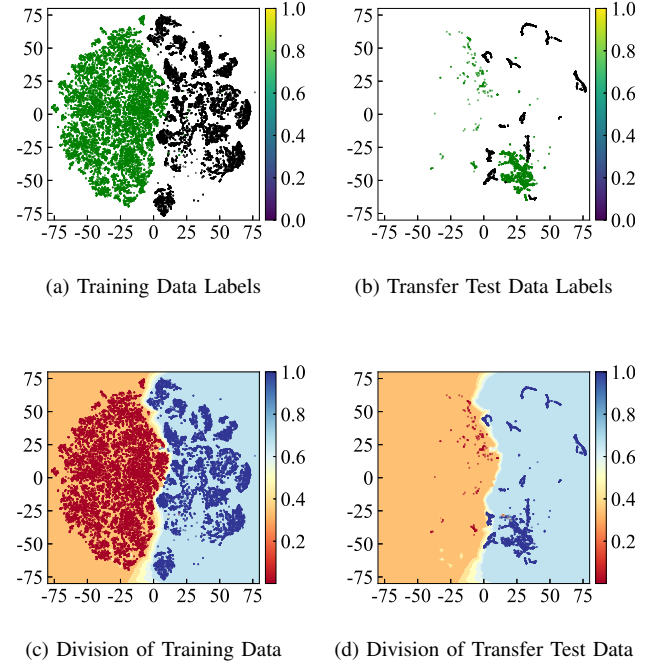
model defined in Eq. 2 can sufficiently describe the transient dynamics [48], [49] of synchronous machines theoretically. The transfer capability of the TTEDNN model is worth investigation. The dataset generated with the rigorous simulation environment can be used to test the transfer capability of the TTEDNN model trained with the second-order simulation environment.

We considered two type of loads, constant impedance and synchronous motors in the simulation environment, respectively. Table III shows the transfer performance for the two types of loads. For the synchronous motor load, the trained TTEDNN model gives 91.07% ACC. For the constant impedance load, the performance of the TTEDNN model drops dramatically to 62.38% ACC. Interestingly, the TTEDNN model has 100% FPR while the FNR is less than 15%. In other words, the TTEDNN model makes the wrong prediction for the 85% of the stable samples and correct prediction for all the unstable samples. Essentially, the TTEDNN model is a classifier extracting features of the input data for distinguishing the stable and unstable samples. The features from the hidden layer of the MLP in the TTEDNN model are visualized in Fig. 5 with the t-Distributed Stochastic Neighbor Embedding (t-SNE) dimensionality reduction technique [50]. The colored dots denote the value of classification confidence, *i.e.*, the sample is stable (unstable) when classification confidence is larger (smaller) than 0.5.

Fig. 5a and Fig. 5c show the features distribution of training dataset labels and predictions, respectively. It can be found in Fig. 5a that the TTEDNN model divide the stable and unstable samples into two clusters with a clear boundary. Clearly, the classification works well on the training dataset. However, as shown in Fig. 5b, when the trained TTEDNN model is directly used for the samples generated with the simulation environment with the constant impedance loads, it fails to divide the stable and unstable samples. The classification results in a large part of stable samples that are mistakenly predicted to be unstable, as shown at the right corner of Fig. 5d. Physically, the loads in the second-order power system model are equivalently synchronous motors in the power system model in the PST module. However, for the constant impedance, its physical characteristics are very different from the synchronous motors in nature, leading to distinct features distributions of the transient dynamics.

## VI. CONCLUDING REMARKS

The TTEDNN model demonstrates robust and outstanding performance to predict the transient stability in power systems. First, the TTEDNN model maps the spatial information of



(c) Division of Training Data (d) Division of Transfer Test Data  
Fig. 5. Visualization of high-dimensions features from the hidden layer with the constant impedance loads. The (a) and (b) are training and transfer test data colored with labels, and (c) and (d) are training and test data colored with network outputs.

power system topology into the GC modules as well as extracts the temporal and topological features from the transient dynamics of power systems with the GC and TC modules. Next, the TTEDNN model outperforms the existing deep learning models on almost all the performance metrics, *e.g.*, it can reach 99.38% (98.60%) ACC and 0.36% (2.56%) FPR under the single-node and multiple-node perturbations in the IEEE 39-bus power system. Third, the TTEDNN model is very efficient, much faster than the conventional TDS method. Fourth, the TTEDNN model has the transfer capability: the trained TTEDNN model with the second-order simulation environment can be directly used to predict the transient stability in the more realistic simulation environment based on the higher-order power system dynamics, especially when loads are synchronous motors. The transfer capability is extremely useful when the high-quality dataset is not available in the real-world power system. The TTEDNN model can be widely applied in transient stability analysis. The transfer learning capability of the TTEDNN model demands more theoretical and practical research in the future.

## REFERENCES

- [1] P. Sarajcev, A. Kunac, G. Petrovic, and M. Despalatovic, "Power system transient stability assessment using stacked autoencoder and voting ensemble," *Energies*, vol. 14, no. 11, 2021.
- [2] J. Hou, C. Xie, T. Wang, Z. Yu, Y. Lü, and H. Dai, "Power system transient stability assessment based on voltage phasor and convolution neural network," in *2018 IEEE International Conference on Energy Internet (ICEI)*, 2018, pp. 247–251.
- [3] S.-G. Yang, B. J. Kim, S.-W. Son, and H. Kim, "Power-grid stability predictions using transferable machine learning," *Chaos: An Interdisciplinary Journal of Nonlinear Science*, vol. 31, no. 12, p. 123127, 2021.

- [4] S. Zhang, Z. Zhu, and Y. Li, "A critical review of data-driven transient stability assessment of power systems: principles, prospects and challenges," *Energies*, vol. 14, no. 21, p. 7238, 2021.
- [5] Z. Liu, X. He, Z. Ding, and Z. Zhang, "A basin stability based metric for ranking the transient stability of generators," *IEEE Transactions on Industrial Informatics*, vol. 15, no. 3, pp. 1450–1459, 2019.
- [6] B. Zhang, X. Jin, S. Tu, Z. Jin, and J. Zhang, "A new fpga-based real-time digital solver for power system simulation," *Energies*, vol. 12, no. 24, p. 4666, 2019.
- [7] T. L. Vu and K. Turitsyn, "Lyapunov functions family approach to transient stability assessment," *IEEE Transactions on Power Systems*, vol. 31, no. 2, pp. 1269–1277, 2015.
- [8] Vu, Thanh Long and Turitsyn, Konstantin, "A framework for robust assessment of power grid stability and resiliency," *IEEE Transactions on Automatic Control*, vol. 62, no. 3, pp. 1165–1177, 2017.
- [9] M. Anghel, F. Milano, and A. Papachristodoulou, "Algorithmic construction of lyapunov functions for power system stability analysis," *IEEE Transactions on Circuits and Systems I: Regular Papers*, vol. 60, no. 9, pp. 2533–2546, 2013.
- [10] R. Yan, G. Geng, Q. Jiang, and Y. Li, "Fast transient stability batch assessment using cascaded convolutional neural networks," *IEEE Transactions on Power Systems*, vol. 34, no. 4, pp. 2802–2813, 2019.
- [11] J. J. Q. Yu, D. J. Hill, A. Y. S. Lam, J. Gu, and V. O. K. Li, "Intelligent time-adaptive transient stability assessment system," *IEEE Transactions on Power Systems*, vol. 33, no. 1, pp. 1049–1058, 2018.
- [12] L. Zhang, G. Wang, and G. B. Giannakis, "Real-time power system state estimation and forecasting via deep unrolled neural networks," *IEEE Transactions on Signal Processing*, vol. 67, no. 15, pp. 4069–4077, 2019.
- [13] K. Simonyan and A. Zisserman, "Very deep convolutional networks for large-scale image recognition," in *International Conference on Learning Representations, ICLR 2015*, 5 2015.
- [14] K. He, X. Zhang, S. Ren, and J. Sun, "Deep residual learning for image recognition," in *Proceedings of the IEEE conference on Computer Vision and Pattern Recognition (CVPR)*, 6 2016, pp. 770–778.
- [15] G. Han, S. Liu, K. Chen, N. Yu, Z. Feng, and M. Song, "Imbalanced sample generation and evaluation for power system transient stability using ctgan," in *International Conference on Intelligent Computing & Optimization*. Springer, 2021, pp. 555–565.
- [16] T. N. Kipf and M. Welling, "Semi-supervised classification with graph convolutional networks," in *5th International Conference on Learning Representations, ICLR*, 2 2017.
- [17] B. Yu, H. Yin, and Z. Zhu, "Spatio-temporal graph convolutional networks: A deep learning framework for traffic forecasting," in *Proceedings of the Twenty-Seventh International Joint Conference on Artificial Intelligence (IJCAI-18)*. International Joint Conferences on Artificial Intelligence Organization, 7 2018, pp. 3634–3640.
- [18] S. Yan, Y. Xiong, and D. Lin, "Spatial temporal graph convolutional networks for skeleton-based action recognition," in *AAAI Conference on Artificial Intelligence*, 4 2018, pp. 7444–7452.
- [19] Z. Wu, S. Pan, F. Chen, G. Long, C. Zhang, and P. S. Yu, "A comprehensive survey on graph neural networks," *IEEE Transactions on Neural Networks and Learning Systems*, vol. 32, no. 1, pp. 4–24, 2021.
- [20] W. Liao, B. Bak-Jensen, J. R. Pillai, Y. Wang, and Y. Wang, "A review of graph neural networks and their applications in power systems," 2021, arXiv: 2101.10025.
- [21] Y. Liu, N. Zhang, D. Wu, A. Botterud, R. Yao, and C. Kang, "Searching for critical power system cascading failures with graph convolutional network," *IEEE Transactions on Control of Network Systems*, vol. 8, no. 3, pp. 1304–1313, 2021.
- [22] I. Goodfellow, Y. Bengio, and A. Courville, *Deep Learning*. MIT Press, 2016.
- [23] A. van den Oord, S. Dieleman, H. Zen, K. Simonyan, O. Vinyals, A. Graves, N. Kalchbrenner, A. Senior, and K. Kavukcuoglu, "Wavenet: A generative model for raw audio," 2016, arXiv: 1609.03499.
- [24] S. Bai, J. Z. Kolter, and V. Koltun, "An empirical evaluation of generic convolutional and recurrent networks for sequence modeling," 2018, arXiv:1803.01271.
- [25] X. Tang, H. Chen, W. Xiang, J. Yang, and M. Zou, "Short-term load forecasting using channel and temporal attention based temporal convolutional network," *Electric Power Systems Research*, vol. 205, p. 107761, 2022.
- [26] D. Li, F. Jiang, M. Chen, and T. Qian, "Multi-step-ahead wind speed forecasting based on a hybrid decomposition method and temporal convolutional networks," *Energy*, vol. 238, p. 121981, 2022.
- [27] F. A. Rodrigues, T. K. D. Peron, P. Ji, and J. Kurths, "The kuramoto model in complex networks," *Physics Reports*, vol. 610, pp. 1–98, 2016.
- [28] G. Filatrella, A. Nielsen, and N. Pedersen, "Analysis of a power grid using a kuramoto-like model," *The European Physical Journal B - Condensed Matter and Complex Systems*, vol. 61, pp. 485–491, 02 2008.
- [29] F. Dörfler, M. Chertkov, and F. Bullo, "Synchronization assessment in power networks and coupled oscillators," in *2012 IEEE 51st IEEE Conference on Decision and Control (CDC)*, 2012, pp. 4998–5003.
- [30] F. Dörfler, M. Chertkov, and F. Bullo, "Synchronization in complex oscillator networks and smart grids," *Proceedings of the National Academy of Sciences of the United States of America*, vol. 110, no. 6, pp. 2005–2010, feb 2013.
- [31] J. Chow and K. Cheung, "A toolbox for power system dynamics and control engineering education and research," *IEEE Transactions on Power Systems*, vol. 7, no. 4, pp. 1559–1564, 1992.
- [32] J. H. Chow and J. J. Sanchez-Gasca, *Power system modeling, computation, and control*. John Wiley & Sons, 2020.
- [33] F. Dorfler and F. Bullo, "Synchronization and transient stability in power networks and nonuniform kuramoto oscillators," *SIAM Journal on Control and Optimization*, vol. 50, no. 3, pp. 1616–1642, 2012.
- [34] L. R. Górgão, B. Schäfer, D. Witthaut, and C. Beck, "Spatio-temporal complexity of power-grid frequency fluctuations," *New Journal of Physics*, vol. 23, no. 7, p. 073016, jul 2021.
- [35] B. Schäfer, C. Beck, K. Aihara, D. Witthaut, and M. Timme, "Non-gaussian power grid frequency fluctuations characterized by lévy-stable laws and superstatistics," *Nature Energy*, vol. 3, no. 2, pp. 119–126, 1 2018.
- [36] J. Dong, J. Zuo, L. Wang, K. Kook, I.-Y. Chung, Y. Liu, S. Affare, B. Rogers, and M. Ingram, "Analysis of power system disturbances based on wide-area frequency measurements," in *2007 IEEE Power Engineering Society General Meeting*, 07 2007, pp. 1–8.
- [37] V. Nair and G. E. Hinton, "Rectified linear units improve restricted Boltzmann machines," in *Proceedings of the 27th International Conference on Machine Learning (ICML-10)*, June 2010, pp. 807–814.
- [38] J. Long, E. Shelhamer, and T. Darrell, "Fully convolutional networks for semantic segmentation," in *Proceedings of the IEEE Conference on Computer Vision and Pattern Recognition (CVPR)*, 2015, pp. 3431–3440.
- [39] J. L. Ba, J. R. Kiros, and G. E. Hinton, "Layer normalization," 2016, arXiv:1607.06450.
- [40] M. Pai, *Energy function analysis for power system stability*. Springer Science & Business Media, 2012.
- [41] A. R. Al-Roomi, "Power Flow Test Systems Repository," Halifax, Nova Scotia, Canada, 2015. [Online]. Available: <https://al-roomi.org/power-flow>
- [42] R. D. Zimmerman, C. E. Murillo-Sánchez, and R. J. Thomas, "Matpower: Steady-state operations, planning, and analysis tools for power systems research and education," *IEEE Transactions on power systems*, vol. 26, no. 1, pp. 12–19, 2010.
- [43] M. Abadi, A. Agarwal, P. Barham, E. Brevdo, Z. Chen, C. Citro, G. S. Corrado, A. Davis, J. Dean, M. Devin, S. Ghemawat, I. Goodfellow, A. Harp, G. Irving, M. Isard, Y. Jia, R. Jozefowicz, L. Kaiser, M. Kudlur, J. Levenberg, D. Mané, R. Monga, S. Moore, D. Murray, C. Olah, M. Schuster, J. Shlens, B. Steiner, I. Sutskever, K. Talwar, P. Tucker, V. Vanhoucke, V. Vasudevan, F. Viégas, O. Vinyals, P. Warden, M. Wattenberg, M. Wicke, Y. Yu, and X. Zheng, "TensorFlow: Large-scale machine learning on heterogeneous systems," 2015, software available from tensorflow.org. [Online]. Available: <http://tensorflow.org/>
- [44] Y. Lecun, L. Bottou, Y. Bengio, and P. Haffner, "Gradient-based learning applied to document recognition," *Proceedings of the IEEE*, vol. 86, no. 11, pp. 2278–2324, 1998.
- [45] S. Woo, J. Park, J.-Y. Lee, and I.-S. Kweon, "CBAM: convolutional block attention module," in *Proceedings of the European conference on computer vision (ECCV)*. European Conference on Computer Vision, 2018, pp. 3–19.
- [46] V. Petar, C. Guillem, C. Arantxa, R. Adriana, L. Pietro, and B. Yoshua, "Graph attention networks," in *International Conference on Learning Representations, ICLR 2018*, 2018.
- [47] D. Grattarola and C. Alippi, "Graph neural networks in tensorflow and keras with spektral [application notes]," *IEEE Computational Intelligence Magazine*, vol. 16, no. 1, p. 99–106, Feb 2021.
- [48] P. J. Menck, J. Heitzig, J. Kurths, and H. Joachim Schellnhuber, "How dead ends undermine power grid stability," *Nature communications*, vol. 5, p. 3969, 2014.
- [49] P. Kundur, *Power system stability and control*. Tana McGraw-Hill Education, 1994.
- [50] L. van der Maaten and G. Hinton, "Visualizing data using t-sne," *Journal of Machine Learning Research*, vol. 9, no. 86, pp. 2579–2605, 2008.